Long range intra-molecular electronic communication in bis-(ferrocenyl-ethynyl) complexes incorporating conjugated heterocyclic spacers: synthesis, crystallography and electrochemistry

Hakikulla H. Shah,[a] RayyaA. Al-Balushi,[a] Mohammed K. Al-Suti,[a] Muhammad S. Khan,[a]* Christopher H. Woodall,[b] Kieran C. Molloy,[b] Paul R. Raithby,[b]* Thomas P. Robinson,[b] Sara E.C. Dale,[b] Frank Marken[b]*

[a]Department of Chemistry, Sultan Qaboos University, P.O. Box 36, Al-Khodh 123, Sultanate of Oman

[b]Department of Chemistry, University of Bath, Bath BA2 7AY, UK.

Abstract

A new series of bis(ferrocenylethynyl) complexes **3-7** and a mono(ferrocenylethynyl) complex **8** have been synthesized incorporating conjugated carbocyclic and heterocyclic spacer groups with the ethynyl group facilitating an effective long range intra-molecular interaction. The complexes were characterized by NMR, IR, and UV-vis spectroscopy as well as X-ray crystallography. Redox properties of these complexes were investigated using cyclic voltammetry and spectroelectrochemistry. Although there is a large separation of ~14Å between the two redox centers, $\Delta E_{1/2}$ values in this series of complexes ranged from 50 to 110 mV. The appearance of IVCT bands in the UV-vis-NIR region for the mono-cationic complexes further confirmed effective intra-molecular electronic communication. Computational studies are presented which show the degree of delocalization across the Fc-C≡C-C≡C-Fc (Fc = $C_5H_5FeC_5H_4$) HOMO.

Keywords: ferrocene, alkynyl, conjugation, electrochemistry, X-ray.

Introduction

There is considerable contemporary interest in metal-containing polymers in which metal centers are linked by conjugated moieties, as these have the potential for facile electron transfer between metals; such species are potential molecular wires, with application in the down-scaling of diverse electronic devices.[1-15] Ferrocene-based materials have been central to this research, as the complexes are often synthetically robust, show well-defined redox chemistry and readily support mixed-valence systems.[16-22] In particular, a wide range of ferrocene moieties linked by conjugated spacers such as alkenes,[16,23-27] alkynes[28] and /or aromatic rings[29-32] have been synthesized and their properties reported. We have a long-standing interest in this general area, and in particular the synthesis and characterization of oligomeric platinum[33-36] and gold[37-40] species linked by alkynes, as these serve as model systems for long chain polymers. In this paper, we turn our attention to related systems in which ferrocene groups are linked by alkyne / heterocyclic spacers, combining synthesis, crystallography and spectroelectrochemical studies. Several previous studies have reported alkyne-bridged mixed valence bis-ferrocene complexes[16,41-50] as well as structural studies of ferrocene groups linked by alkynes and/or oligothiophenes, fluorenes or similar heterocycles.[31,51-53]

We have synthesized a new series of bis(ferrocenylethynyl) complexes **3-7** and a mono(ferrocenylethynyl) complex **8** incorporating novel heterocyclic spacer groups. Heterocyclic spacer groups –quinoline and benzothiadiazole - have been utilized for complexes **3** and **4**, respectively. These spacers have been fruitfully used as such and in substituted forms for development of sensors, taking advantage of the conjugated framework.[54-60] Heterocyclic spacers such as phenyl-substituted thieno[3,4-b]pyrazine have shown to be excellent precursors for the production of low band gap conjugated polymers[61-63] and have been utilized for the synthesis for

complexes **5** and **6**. Similarly, fused thiophenes show better conjugation than their non-fused analogues[64] and thus are used for the synthesis of complexes **7** and **8**. Combining the conjugation properties of the spacers and connecting them to a terminal ferrocene *via* a rigid rod such as an alkyne should enhance the electronic communication between the two metal centers.

Herein we report the synthesis, characterization and electrochemical studies of the complexes **2-8** along with X-ray crystallographic studies of the complexes **2**, **4-6** and **8**. The effect of the different spacer groups on the redox property of the ferrocene is investigated by cyclic voltammetry. The signatures of the mono-cationic species formed during the long range intra-molecular interaction of the ferrocene units are studied by spectro-electrochemistry and pure spectra for the mono-cations are established with the help of spectral deconvolution. Interaction parameters such as ferrocene-to-ferrocene distance, the separation of the ferrocene reversible potentials, and the features of the inter-valence charge transfer (IVCT) band are discussed.

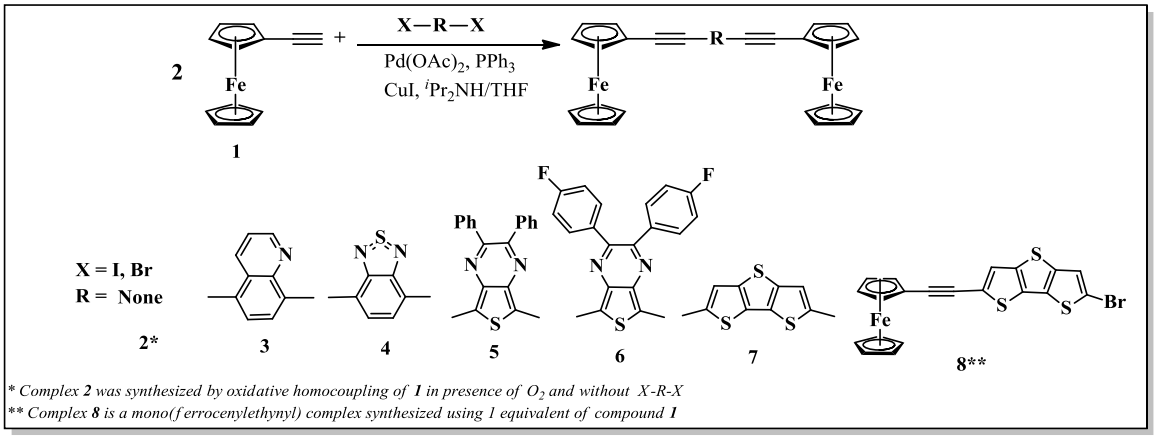

Scheme 1. Synthesis of bis(ferrocenynyethynyl) complexes **2-7** and monoferrocenylethynyl complex **8**

Experimental

All reactions were carried out under inert atmosphere using Schlenk techniques. Solvents were pre-dried and distilled from appropriate drying agents. All chemicals, unless otherwise stated, were obtained from commercial sources and used as received. Preparative TLC was performed on 0.7 mm silica plates. The key starting material ethynylferrocene was synthesized by adaptation of a literature method[25,65,66]. The NMR spectra were recorded on a Bruker AM-400 spectrometer in $CDCl_3$. The ^1H NMR spectra were referenced to solvent resonances. IR spectra were recorded as CH_2Cl_2 solutions, in a NaCl cell, on a Nicolet-Impact 400D FT-IR spectrometer, mass spectra on a Kratos MS 890 spectrometer by the electron impact (EI) and fast atom bombardment (FAB) techniques. Microanalyses were performed in the Department of Chemistry, University of Bath, UK. Computations were performed on the University of Bath's High Performance Computing Facility. Column chromatography was performed either on Kieselgel 60 (230 – 400 mesh) silica gel or alumina (Brockman Grade II-III).

Synthesis

Ethynylferrocene[65] **(1).** Acetylferrocene 2.14 g (10 mmol) and triphenylphosphine 10.48 g (40 mmol) in anhydrous acetonitrile (20 ml) at 0°C under argon atmosphere was added to 3.08 g (20 mmol) of tetrachlormethane in one portion. The mixture was warmed to room temperature. Stirring was continued for 45 minutes and then 5 ml distilled water was added to the solution. The mixture was extracted with ether (50 ml x 3), washed with brine and then dried over anhydrous magnesium sulphate ($MgSO_4$). Solvent was evaporated and the residue was dissolved in dichloromethane and filtered through a plug of alumina. After removal of the solvent under reduced pressure, a red crystalline intermediate compound was obtained in 85 % yield (2.4 g). 1.68 g (6 mmol) of this intermediate compound in 10 ml dry THF at 0 °C was added to 8 mL (12

mmol) of ^{n}BuLi (1.5 M in THF) under rigorous stirring for 10 minutes. The reaction mixture was warmed to room temperature and stirring was continued for 15 minutes followed by hydrolysis with 10 ml of distilled water and stirred for another 10 minutes. The mixture was extracted with ether (50 ml x 3) and the combined organic layer was dried over $MgSO_4$. After filtration through a plug of alumina and removal of solvent under reduced pressure the titled compound **1** was obtained as red crystalline solid in 93% yield (1.1 g). IR (CH_2Cl_2): 2110 cm^{-1} ν(C≡C); 3301 cm^{-1} ν(C≡C-H). ^{1}H NMR (300 MHz, $CDCl_3$): δ =4.21 **(s,** 5H), 4.19(t, 2H), 4.47(t, 2H) and 2.71(s, 1H). FABMS: m/z 211 (M^+). $C_{12}H_{10}Fe$. Calc.: C, 68.62; H, 4.80%; Anal. Found: C, 68.53; H, 4.86%

Fc–C≡C–C≡C–Fc (2). Ethynylferrocene (0.105 g, 0.50 mmol) and di-*iso*propylamine (5 ml) were mixed with catalytic amounts of $Pd(OAc)_2$ (2 mg), CuI (2 mg) and PPh_3 (5 mg). The mixture was allowed to reflux for 15 h under aerobic conditions, after which all volatile components were removed under reduced pressure. The residue was dissolved in CH_2Cl_2 and chromatographed through a silica column using hexane-CH_2Cl_2 (1:1, v/v) as eluent. The titled compound was obtained as a dark red powder in 95% yield (0.20 g). IR (CH_2Cl_2): 2148 cm^{-1} ν(C≡C). ^{1}H NMR (300 MHz, $CDCl_3$): δ = 3.94 (t, 4H, J=1.7 Hz, Cp), 4.13 (s, 10H, Cp), 4.46 (t, 4H, J=1.9 Hz, Cp) ppm. FABMS: m/z 419 (M^+).$C_{24}H_{18}Fe_2$ Calc.: C, 68.95; H, 4.34%; Anal. Found: C, 68.99; H, 4.29%.

Fc–C≡C–R–C≡C–Fc (R =Quinoline-5,8-diyl) (3). Under argon atmosphere, a solution of ethynylferrocene (0.23 g, 1.1 mmol) and 5,8-diiodoquinoline[67] (0.14 g, 0.5 mmol) in di-*iso*propylamine (15 ml) were mixed with catalytic amounts of $Pd(OAc)_2$ (3 mg), CuI (3 mg) and

PPh_3 (10 mg). The mixture was allowed to reflux for 24 h, after which all volatile components were removed under reduced pressure. The residue was dissolved in CH_2Cl_2 and chromatographed through a silica column using hexane-CH_2Cl_2 (2:1, v/v) as eluent. The titled compound was obtained as a dark red power in 53% yield (0.29 g). IR (CH_2Cl_2): 2188 cm^{-1} ν(C≡C). ^{1}H NMR (300 MHz, $CDCl_3$): δ = 4.11 (pseudo-t, 4H, Cp), 4.31 (s, 10H, Cp), 4.62 (pseudo-t, 4H, Cp), 6.94 (dd, 1H, J = 12.1 Hz, spacer), 7.58 (d, 1H, J = 7.5 Hz, spacer), 7.84 (d, 1H, J = 7.9 Hz, spacer), 8.77 (d, 1H, J = 8.3 Hz, spacer), 8.92 (dd, 1H, J = 6.0 Hz, spacer).FABMS: m/z 546 (M+). $C_{33}H_{23}Fe_2N$Calc.: C, 72.89; H, 4.25%;Anal. Found: C, 72.98; H, 4.29%.

Fc–C≡C–R–C≡C–Fc (R =Benzothiadiazole-4,7-diyl) (4). The titled bis(ferrocenylethynyl) compound was prepared by following similar procedure as described above for **3** using ethynylferrocene (0.23 g, 1.1 mmol) and 4,7-dibromobenzothiadiazole[67] (0.14 g, 0.5 mmol) giving a brown solid in 82% yield (0.45 g). IR (CH_2Cl_2): 2184 cm^{-1} ν(C≡C). ^{1}H NMR (300 MHz, $CDCl_3$):δ =4.04 (t, 4H, J=3.4 Hz, Cp), 4.26 (s, 10H, Cp), 4.59 (pseudo-t, 4H, J=3.8 Hz, Cp),7.30 (d, 2H, J = 7.5 Hz, spacer). FABMS: m/z 553 (M^+). $C_{30}H_{20}Fe_2N_2S$ Calc.: C, 65.25; H, 3.65%.Anal. Found: C, 65.31; H, 3.71%.

Fc–C≡C–R–C≡C–Fc (R = Diphenylthienopyrazine-5,7-diyl) (5). The titled bis(ferrocenylethynyl) compound was prepared by similar procedure to that described for 3 using ethynylferrocene (0.23 g, 1.1 mmol) and 5,7-dibromodiphenylthienopyrazine[68] (0.22 g, 0.5 mmol) to obtain a dark violet powder in 72% yield (0.51 g). IR (CH2Cl2): 2199 cm^{-1} ν(C≡C). ^{1}H NMR (300 MHz, CDCl3): δ =4.04 (pseudo-t, 4H, J=3.4 Hz, Cp), 4.26 (s, 10H, Cp), 4.59

(pseudo-t, 4H, J=3.8 Hz, Cp), 7.40 (m, 2H, J=4.9 Hz, spacer), 7.60-7.63 (m, 8H, spacer)ppm. FABMS: m/z 705 (M+). $C_{42}H_{28}Fe_2N_2S$Calc.: C, 71.61; H, 4.01%.Anal. Found: C, 71.68; H, 4.06%.

Fc–C≡C–R–C≡C–Fc (R = Difluorodiphenylthienopyrazine-5,7-diyl) (6). The titled bis(ferrocenylethynyl) compound was prepared by similar procedure to that described for **3** using ethynylferrocene (0.23 g, 1.1 mmol) and 5,7-dibromo(difluorodiphenyl)thienopyrazine[68] (0.24 g, 0.5 mmol) to obtain a dark violet powder in 74% yield (0.55 g). IR (CH_2Cl_2): 2199 cm^{-1} ν(C≡C). ^1H NMR (300 MHz, CDCl3): δ =4.04 (pseudo-t, 4H, J=3.4 Hz, Cp), 4.26 (s, 10H, Cp), 4.59 (pseudo-t, 4H, J=3.8 Hz, Cp), 6.74 (dd, 4H, J=8.7 Hz, spacer), 7.33 (dd, 4H, J = 7.3 Hz, spacer) ppm. FABMS: m/z 741 (M^+). $C_{42}H_{26}F_2Fe_2N_2S$ Calc.: C, 68.13; H, 3.54%.Anal. Found: C, 68.78; H, 3.49%.

Fc–C≡C–R–C≡C–Fc(R = Dithienothiophene-2,5-diyl) (7). The titled bis(ferrocenylethynyl) compound was prepared by similar procedure to that described for **3** using ethynylferrocene (0.23 g, 1.1 mmol) and 2,5-dibromodithienothiophene[40] (0.16 g, 0.50 mmol) to obtain an orange powder in 68 % yield (0.21 g). IR (CH_2Cl_2): 2199 cm^{-1} ν(C≡C). ^1H NMR (300 MHz, $CDCl_3$): δ =4.28 (s, 10H, Cp), 4.30 (pseudo-t, 4H, J=3.4 Hz, Cp), 4.55 (pseudo-t, 4H, J=3.8 Hz, Cp), 7.39 (s, 2H, spacer), FABMS: m/z 612 (M^+). $C_{32}H_{20}Fe_2S_3$ Calc.: C, 62.76; H, 3.29%.Anal. Found: C, 62.78; H, 3.19%.

Fc–C≡C–R (R = 5-Bromodithienothiophene-2-yl) (8). The titled mono(ferrocenylethynyl) compound was prepared by reacting ethynylferrocene (0.23 g, 1.1 mmol) and 2,5-

dibromodithienothiophene (0.33 g, 1.0 mmol) at 60 °C for 12 hrs to obtain orange crystals in 54% yield (0.27 g). IR (CH_2Cl_2): 2199 cm^{-1} ν(C≡C). ^{1}H NMR (300 MHz, $CDCl_3$): δ =3.95 (pseudo-t, 2H, J=3.8 Hz, Cp), 4.11 (s, 5H, Cp), 4.46 (pseudo-t, 2H, J=3.8 Hz, Cp), 6.62 (s, 1H, spacer), 7.13 (s, 1H, spacer). FABMS: m/z 483 (M^+). $C_{20}H_{11}BrFeS_3$ Calc.: C, 49.71; H, 2.29%.Anal. Found: C, 49.78; H, 2.19%.

Crystallography

Single-crystal X-ray diffraction experiments were performed at 150(2) K on either an Oxford Diffraction Gemini A Ultra CCD diffractometer (5, 6, 8) or an Nonius Kappa CCD diffractometer (**2**, **4**) using monochromatic Mo K_α radiation (λ=0.71073 Å). For **5**, **6**, **8**, the sample temperature was controlled using an Oxford Diffraction Cryojet apparatus; CrysAlis Pro was used for the collection of frames of data, indexing reflections and determining lattice parameters. For **2**, **4** temperature control was made using an Oxford Cryostream device. A multi-scan absorption correction was applied in all cases. Structures were solved by direct methods using SHELXS-86[69] and refined by full-matric least-squares on F^2 using SHELX-97.[70] Crystallographic data for all complexes studied can be found in Table 1.

Table 1. Crystallographic data for **4** – **6**, **8**.

	4	**5**	**6**	**8**
Empirical formula	$C_{30}H_{20}Fe_2N_2S$	$C_{42}H_{28}Fe_2N_2S$	$C_{42}H_{26}F_2Fe_2N_2S$	$C_{20}H_{11}BrFeS_3$
Formula weight	552.24	704.42	740.41	483.23
Crystal system	Monoclinic	Triclinic	Triclinic	Triclinic
Space group	C2/c	P -1	P -1	P -1
a	30.6586(3)	7.6536(5)	7.4305(5) Å	7.867(5)
b	9.8566(1)	12.7415(7)	13.2951(6	10.000(5)
c	21.6227(3)	16.5787(11)	16.4962(10)	11.548(5)
α		100.757(5).	82.729(4)	77.054(5)
β	134.389(1)	97.360(6)	85.045(5)	86.042(5)
γ		92.718(5).	80.538(5)°.	87.945(5)°.
Volume ($Å^3$)	4669.35(9)	1571.00(17)	1590.97(16)	883.1(8)
Z	8	2	2	2
ρ_{calc} ($Mg/m^{3)}$	1.571	1.489	1.546	1.817
μ(Mo-K_α) (mm^{-1})	1.355	1.025	1.025	3.470
F(000)	2256	724	756	480
Crystal size (mm)	0.20 x 0.16 x 0.16	0.4 x 0.2 x 0.05	0.30 x 0.30 x 0.10	0.3 x 0.2 x 0.1
Theta range (^{o})	4.14 to 25.35°.	2.81 to 26.37°.	2.79 to 24.71°.	3.06 to 29.61°.
Reflections collected	38948	13087	14712	15957
Independent refl'ns [R(int)]	4258 [0.0431]	6388 [0.0603]	5432 [0.0599]	4434 [0.0450]
Max. and min. transmission	0.879, 0.805	1.000, 0.873	1.000, 0.882	1.000, 0.758
Goodness-of-fit on F^2	1.155	0.981	1.102	0.955
Final R_1, wR_2 [I>2σ (I)]	0.0368, 0.1040	0.0537, 0.1021	0.0615, 0.1640	0.0422, 0.1020
Final R_1, wR_2 (all data)	0.0452, 0.1092	0.0888, 0.1178	0.0777, 0.1780	0.0684, 0.1165
Largest diff. peak, hole ($eÅ^3$)	0.515, -0.914	0.639,-0.422	1.119, -0.870	0.788,-0.763

Electrochemistry

Cyclic voltammograms were recorded in a dried glass cell purged with purified argon. A 3 mm diameter platinum disc electrode was used as working electrode and a Pt-wire served as counter electrode, while a KCl-saturated calomel electrode (Radiometer Ref 401) served as the reference electrode. Under these conditions the reversible potential forferrocene is $E_{1/2}$= 0.527 V. Electrolyte solutions were prepared from dichloroethane (DCE) and [*n*-Bu_4N][PF_6] (Fluka, dried in oil-pump vacuum) as supporting electrolyte. The respective organometallic complexes were added at ca. 1 mM concentration. Cyclic voltammograms were recorded using a micro Autolab III (Ecochemie, The Netherlands). Digisim version 2.0 was employed to simulate cyclic voltammetry data.

Spectro-electrochemistry

Spectro-electrochemistry was performed in a home-built optically transparent thin layer electrolysis (OTTLE) cell by laminating a Ag wire (reference), Pt-Mesh (10 mm x 7.5 mm, working) and Pt- wire (auxiliary).[71] The electrode was used in a 0.1 cm path length quartz UV-vis cell. Spectra were recorded with reference to the spectrum of the pure solvent by carrying out an initial baseline correction without any potential applied to the solvent-filled cell. UV-vis spectra were then recorded with compounds dissolved in DCE with [*n*-Bu_4N][PF_6] at different applied potentials. UV-vis data were obtained at a rate of 600 nm min^{-1}. For each measurement, the potential of the OTTLE cell was kept at a constant value and the absorbance spectrum of the solution was recorded between 200 nm and 1100nm. Data analysis was based on principle component analysis programmed in MATLAB (version 2010b, Mathwork, Inc.). The equation $\hat{X} = \hat{C} \bullet \hat{S} + \hat{E}$ was used with $\hat{X}$, the experimental spectra matrix at three selected potentials, $\hat{C}$,

the concentration coefficients, $\hat{S}$, the pure component spectra, and $\hat{E}$, the error matrix to be minimised forthe deconvolution into the pure spectra.[72-74]

Results and Discussion

Synthesis and spectroscopic characterization

The key starting material for the *bis*-(ferrocenylethynyl) compounds, ethynylferrocene(**1**), was prepared in good yield by adaptation of a literature procedure by Luo et al[65] in preference to other reported synthetic methods for this compound[25,66]. The dibromo/diiodo aromatic/hetero-aromatic precursors for **3-7** were prepared as reported previously.[40,67,68,75] The syntheses of **2**–**8** are shown in Scheme 1. The cross-coupling reactions between ethynylferrocene and dibromo/diiodo aromatic/hetero-aromatics in a 2:1 stoichiometry, in $^{i}Pr_2NH$-CH_2Cl_2, in the presence of a Pd(II)/Cu(I) catalyst readily gave the bis(ferrocenylethynyl) compounds (**3-7**) while the oxidative homo-coupling of **1** under aerobic condition yielded complex **2**. Complex **8** was synthesized by 1:1 reaction between **1** and 2,5-dibromodithienothiophene using a lower reaction temperature (60 °C) and a shorter reaction time (12 h). The products of cross-coupling and homo-coupling reactions were purified by silica gel column chromatography giving orange-red crystals (**2, 4** and **8**) and dark blue/black crystals (**5, 6**) in respectable yields (50 - 90 %). All bis(ferrocenylethynyl) complexes (**2-7**) and the monoferrocenylethynyl complex **8** are indefinitely stable to light and air at ambient temperature and were fully characterized by IR, NMR spectroscopy, FAB mass spectrometry, as well as by satisfactory elemental analysis.

The IR spectra of the *bis*-(ferrocenylethynyl) complexes show a single, sharp $\nu_{(C\equiv C)}$ in the 2200 - 2010 cm^{-1} range, characteristic of other ethynylferrocenyls[42,43,76] containing aromatic and hetero-

aromatic spacer groups. The ^{1}H NMR spectra showed a characteristic pattern of singlet and triplet absorption at ~4 ppm for the unsubstituted and substituted cyclopentadienyl protons, respectively. The aromatic and hetero-aromatic spacers gave signals in the 7 - 8 ppm regions as singlet, doublets, dd, and complex multiplets as expected. Mass spectra (+ve FAB) displayed the presence of molecular ions with characteristic fragmentation patterns for the complexes. The structures of the complexes **2**, **4**-**6** and **8** were confirmed by X-ray crystallography.

The electronic absorption spectra of the complexes **2-8** were recorded in CH_2Cl_2 (Table 2). Each compound displays three sets of absorption bands. Bands with λ_{max} below 400 nm can be attributed to a π - π^* transition associated with the organic spacer group. A weak absorption bands at ~450 nm is assigned to Fe^{II} *d-d* transition,[15b] but is overlapped by the strong, broad higher energy peaks ~400 nm arising from π - π^* transition associated with the organic spacer group.

Table 2. UV-vis spectral and spectro-electrochemical results for neutral and mono-cationic forms of **1** – **8** in dichloroethane.

	[Complex] λ_{max}/ nm	$[Complex]^{+}\lambda_{max}$/ nm
1	267, 399 , 514	
2	283, 323, 466	309, 395, 551, 766[a]
3	246, 282, 350, 468	268, 294, 340, 433, 568, 867[a]
4	292, 366, 457	299, 391, 564, 786[a]
5	281, 338	308, 491, 515, 677
6	316, 382	268, 297, 407, 501

7	322, 370, 396, 478	265, 302, 342, 510, 1020[a]
8	261, 363, 466	284, 308, 417, 563, 760[b]

[a]Spectroscopic data for the IVCT band, [b]Spectroscopic data for MLCT band.

Structural Studies

The structures of **4** – **6** and **8** are shown in Figures 1 - 4, respectively, along with selected geometric data. Room temperature data for **2** have been reported previously,[45,42] but our low temperature data are included in Table 3 for direct comparison across the range of structures at a constant temperature. In **2**, the two ferrocenyl units are linked by a -C≡C-C≡C- spacer leading to a Fe...Fe separation of 9.5965(5) Å; the two ferrocenyl groups are disposed in an *anti*- manner with respect to each other at the termini of the conjugated alkynes. The C≡C bond is the longest [1.201(3) Å] seen in this study (Table 3), and is accompanied by a C-C single bond between alkynes [1.374(4) Å] which is the shortest observed, though the other structures reported herein have the Fc-C≡C bonded to a heterocycle, not another alkyne [Fc = $(C_5H_5)Fe(C_5H_4)$]. These bond lengths suggest some delocalization along the C≡C-C≡C unit. The -C≡C-C≡C- unit is essentially linear, with only minor deviations from ideal bond angles of 180 ^{o}at the *sp* carbons (Table 3); the -C≡C-C≡C- torsion angle is -8.7 ^{o}. The C_5H_4 unit connected to this latter fragment is close to being co-planar with it [torsion angle between C_5H_4 and C-C≡C 178.84(17) ^{o}], and the exocyclic Fc -C(≡C)bond length [1.428(3) Å], comparable with the C-C bond lengths within the Cp ring, also suggests some degree of multiple bond character.

Table 3. Comparison of key structural data for the Fc-C≡C-C unit of **2**, **4** – **6, 8**

	C≡C (Å)	Fc-C(≡C) (Å)	(C≡)C-C(Å)	∠ Fc-C≡C-C (^{o})	Fe…Fe(Å)
2[a]	1.201(3)	1.428(3)	1.374(4)	178.7(2), 179.8(3)	9.5965(5)
4	1.186(3)	1.432(3)	1.438(3)	177.4(3), 178.1(3)	13.4942(5)
	1.187(3)	1.430(4)	1.432(8)	171.1(3), 179.4(4)	
5	1.191(5)	1.439(5)	1.414(5)	175.9(4), 174.3(4)	13.0742(11)
	1.189(4)	1.439(5)	1.426(5)	179.9(4), 175.5(4)	
6	1.192(7)	1.431(7)	1.406(7)	176.4(5), 175.5(5)	13.2918(12)
	1.190(7)	1.429(7)	1.425(7)	176.3(5), 176.2(6)	
8	1.182(5)	1.435(5)	1.426(5)	179.7(4), 176.6(4)	-

[a] Data collected at 150 K as part of this work. Room temperature data are given in refs. 45,51

In **4**, the two alkynes in **2** are further separated by a benzothiadiazole-4,7-diyl spacer, increasing the Fe…Fe separation to 13.4942(5) Å (Fig. 1a). While the exocyclic bond between C_5H_4 and C≡C remains the same as in **2** [C(6)-C(11), C(21-C20): 1.432(3), 1.430(4) Å, respectively], the C≡C appears to shorten [1.186(3), 1.187(3) Å] but just remains within ± 3σ of the analogous bond length in **2**. However, the bond at the other end of the alkyne [C(12)-C(13), C(16)-C(19): 1.438(3), 1.432(8) Å, respectively] are lengthened with respect to **2**, and collectively the data suggest a more localized C≡C which retains some possible conjugation with the organometallic fragment but less so with the heterocycle. This asymmetry is also manifest in the angular distortion at C(19) [171.1(3)^o]. Moreover, the orientation of the two Fc units with respect to each other also differs markedly from **2**. While each Fc remains co-planar with C≡C [torsion ∠C(8)-C(7)-C(6)-C(11) -179.9 ^{o}; torsion ∠C(23)-C(22)-C(21)-C(20) -178.9 ^{o}], the two Fc units are close to orthogonal to each other [torsion angle between C_5H_4 planes C(6)-C(10) and C(21)-C(25) = 108.74(12) ^{o}] implying any conjugation is with differing components of the π-manifold at either end of the molecule. The benzothiadiazole heterocycle is planar and co-planar with the

C(6)-C(10) ring of Fc(1), but twisted out of conjugation with Fc(2). In addition, there is a distinct curvature of the C≡C-Fc(2) fragment upwards from the plane of the heterocycle (a feature also seen in **6** and **7** but not **5;** see below). This difference may arise from the fact that there are close S….N contacts between pairs of molecules (Fig. 1b; S(1)…N(1): 3.098(2) Å], though the planes of the two heterocycles are offset (Fig. 2c).

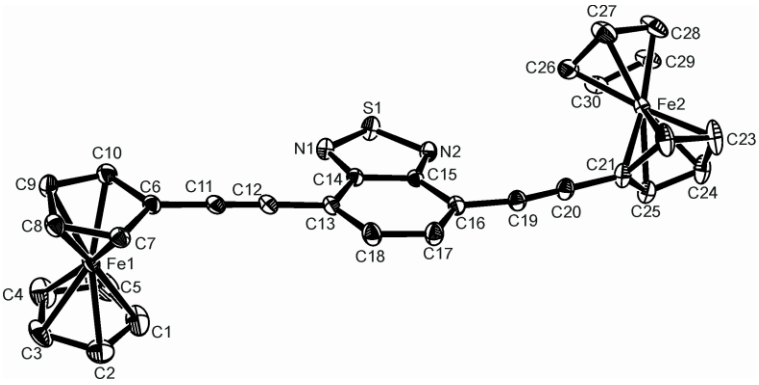

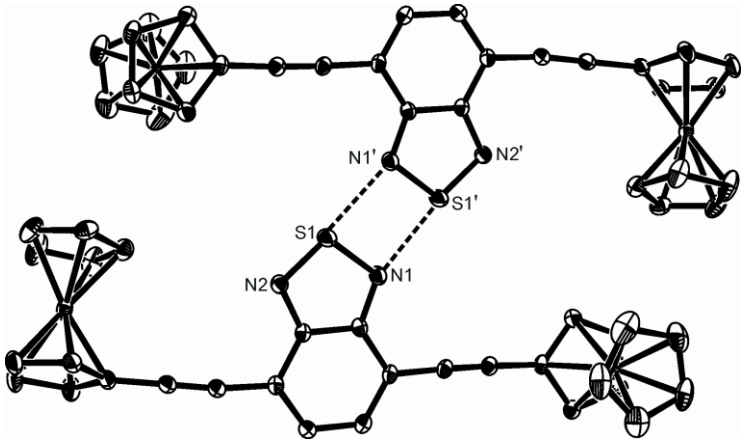

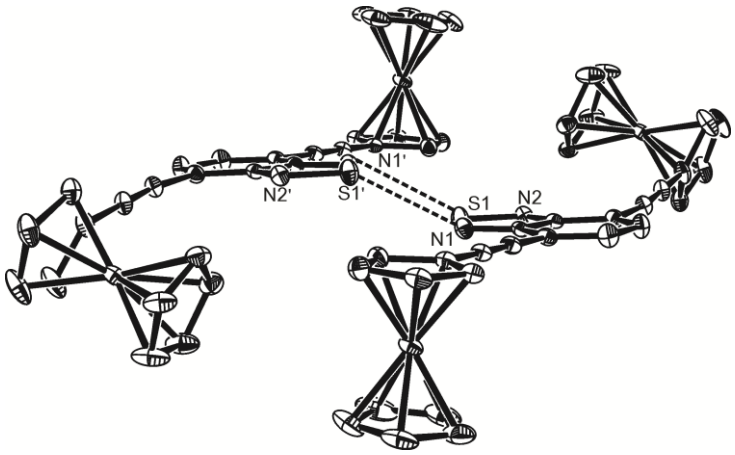

Figure 1. The structure of **4** showing (a, top) the asymmetric unit and the labeling scheme used in the text, (b, middle) dimerization *via* short N..S contacts and (c, bottom) the off-set in heterocycle stacking; thermal ellipsoids are at the 30% level. Selected geometric data: Fe(1)-C(1,5) ring centroid 1.6558(13), Fe(1)-C(6,10) ring centroid 1.6440(11), Fe(2)-C(21,25) ring centroid 1.6470(15), Fe(1)-C(26,30) ring centroid 1.6570(15), C(6)-C(11) 1.432(3), C(11)-C(12) 1.186(3), C(12)-C(13) 1.438(3), C(16)-C(19) 1.432(3), C(17)-C(18) 1.414(4), C(19)-C(20) 1.187(3), C(20)-C(21) 1.430(4), N(1)-S(1) 1.616(2), N(2)-S(1) 1.613(2), C(14)-N(1) 1.343(3), C(14)-C(15) 1.430(3), C(15)-N(2) 1.346(3), S(1)-N1') 3.098(2) Å; C(12)-C(11)-C(6) 177.4(3), C(11)-C(12)-C(13) 178.1(3), C(20)-C(19)-C(16) 171.1(3), C(19)-C(20)-C(21) 179.5(4) ^{o}.

Structures of **5** (Fig. 2) and **6**(Fig. 3a) are related to that of **4** but now incorporate a thienopyrazine spacer substituted at the 5,6-positions of the pyrazine ring; in **4** the alkyne is bonded to the six-membered ring while in **5**and**6** it is bonded to the smaller ring. The fused five- and six-membered rings common to **4 - 6** have similar dimensions, and although the alkynes are linked differently between the two systems this has little impact on the Fe…Fe separation [**4**: 13.4942(5); **5**: 13.0742(11); **6**: 13.2918(12) Å]. It should, however, be noted that, in solution, free rotation about the Fc -C(≡C) bond will lead to a variety of Fe..Fe distances. The key bond

lengths within the Fc-C≡C-C unit (Figure captions, Table 3 are the same within experimental error as those for **4**, but there are differences in the spacial orientation of the Fc units with respect to each other. Thus, in **5** the two Fc units are *anti* across the extended -C≡C-(Het)-C≡C moiety (as seen in **2**), while in **6** they approach orthogonality [torsion angle between C_5H_4 planes C(6)-C(10) and C(19)-C(23) = 80.1(2) ^{o}] similar to **4**; this has the effect of making the Fe…Fe separation marginally shorter than in **6**. The lattice structure of **6** (Fig. 3b) shows short F…S contacts [F(1)…S(1): 3.315(3) Å] and π-stacking of heterocycles in a head-to-tail manner with an inter-plane separation of *ca*. 4 Å [plane centroid to plane = 3.681(4) Å]. In contrast, there are no close intermolecular contacts of any significance in **5** [shortest, C(9)-H(1)…N(2): 2.650 Å**]**, and although pairs of molecules stack with a separation of *ca*. 4 Å [plane centroid to plane = 4.087(2) Å] the two heterocycles are significantly offset with respect to each other.

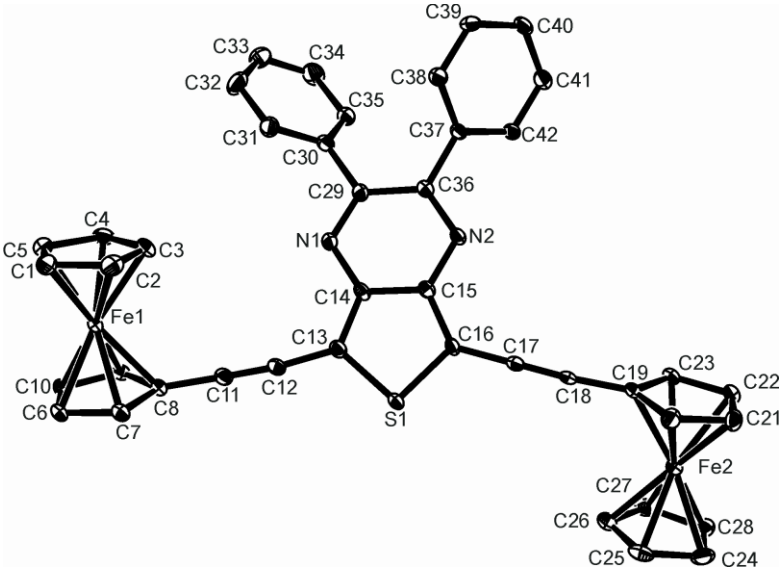

Figure 2. The structure of **5** showing the asymmetric unit and the labeling scheme used in the text; thermal ellipsoids are at the 30% level. Selected geometric data: Fe(1)-C(1,5) ring centroid 1.6477(19), Fe(1)-C(6,10) ring centroid 1.6422(18), Fe(2)-C(19,23) ring centroid 1.6455(18), Fe(1)-C(24,28) ring centroid 1.6475(18), C(8)-C(11) 1.439(5), C(11)-C(12)

1.191(5), C(12)-C(13) 1.414(5), C(16)-C(17) 1.426(5), C(17)-C(18) 1.189(4), C(18)-C(19) 1.439(5), C(16)-S(1) 1.724(3), C(13)-S(1) 1.727(4), C(14)-N(1) 1.370(4), C(14)-C(15) 1.431(4), C(15)-N(2) 1.371(4), C(15)-C(16) 1.394(5) Å; C(12)-C(11)-C(8) 175.9(4), C(11)-C(12)-C(13) 174.3(4), C(18)-C(17)-C(16) 179.9(4), C(17)-C(18)-C(19)175.5(4) ^{o}.

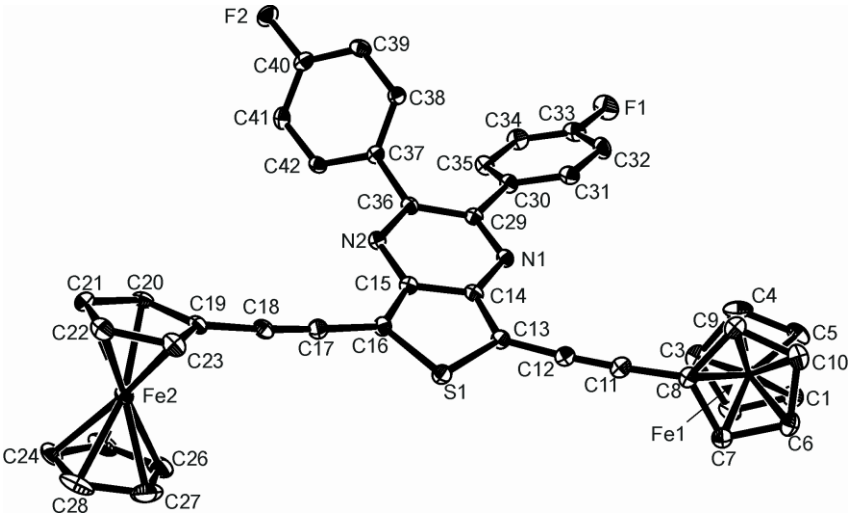

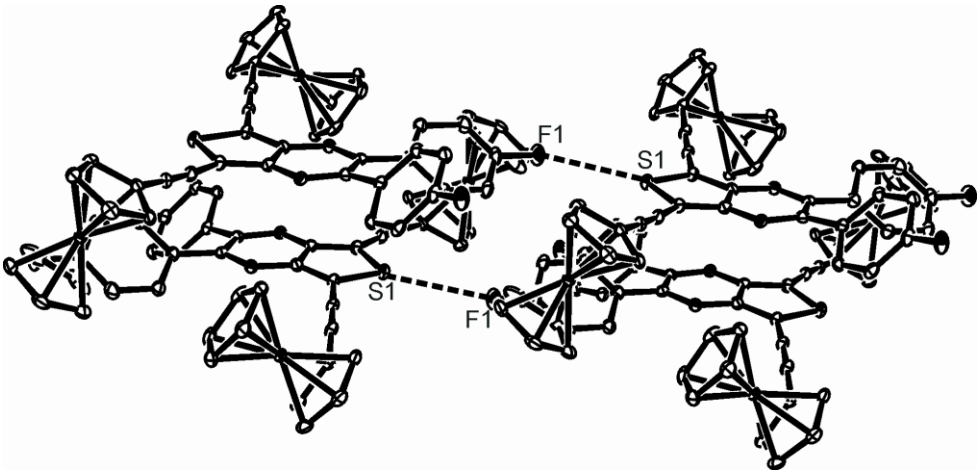

Figure 3. The structure of **6** showing(a, top) the asymmetric unit and the labeling scheme used in the text and (b, bottom) dimerization *via* F…S contacts; thermal ellipsoids are at the 30% level. Selected geometric data: Fe(1)-C(1,5) ring centroid 1.646(2), Fe(1)-C(6,10) ring

centroid 1.647(2), Fe(2)-C(19,23) ring centroid 1.639(2), Fe(1)-C(24,28) ring centroid 1.645(3), C(8)-C(11) 1.431(7), C(11)-C(12) 1.192(7) C(12)-C(13) 1.406(7), C(16)-C(17) 1.425(7), C(16)-S(1) 1.717(5), C(17)-C(18) 1.190(7), C(18)-C(19) 1.429(7), C(13)-S(1) 1.721(4), C(16)-S(1) 1.717(5), C(14)-N(1) 1.368(6), C(15)-N(2) 1.356(6), F(1)…S(1') 3.315(3) Å; C(12)-C(11)-C(8) 176.4(5), C(11)-C(12)-C(13) 175.5(5), C(18)-C(17)-C(16) 176.3(5), C(17)-C(18)-C(19) 176.2(6) ^{o}. Symmetry operation: x, y-1, z.

The structure of **8** (Fig. 4a) has the Fc unit linked *via* the alkyne to a 5-bromodithienothiophene-2-yl fused tri-cycle. The key bond distances and angles (Figure caption) are similar to the structures already described (Table 3). The Fc ring is orthogonal to the heterocycle [torsion angle between C(6)-C(10) ring and the best plane through the heterocycle = 85.21(11) ^{O}] so that the organometallic and heterocycle units conjugate with different π-components of the alkyne, as seen in **2** and **6**. The lattice of **8** reveals short S…S contacts [S(1)…S(2') 3.322(4) Å] generating dimers which stack with heterocycles head-to-tail with each other [Fig. 4b; plane centroid to plane = 3.469(2) Å]. There is also a visible curvature of the C≡C-Fc moiety away from the plane of the heterocycle, as seen also in **4** and **6**.

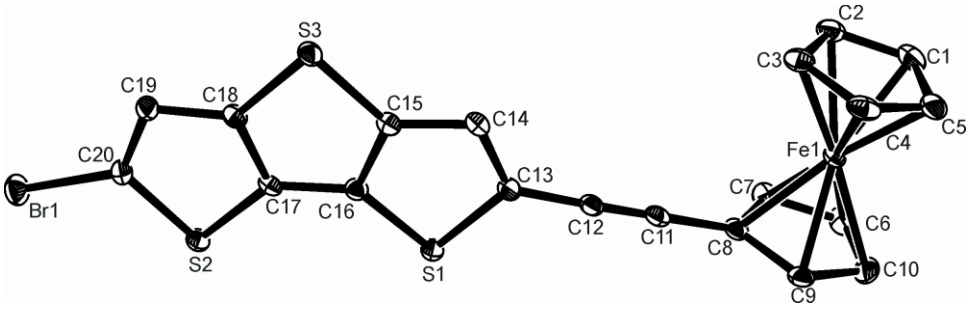

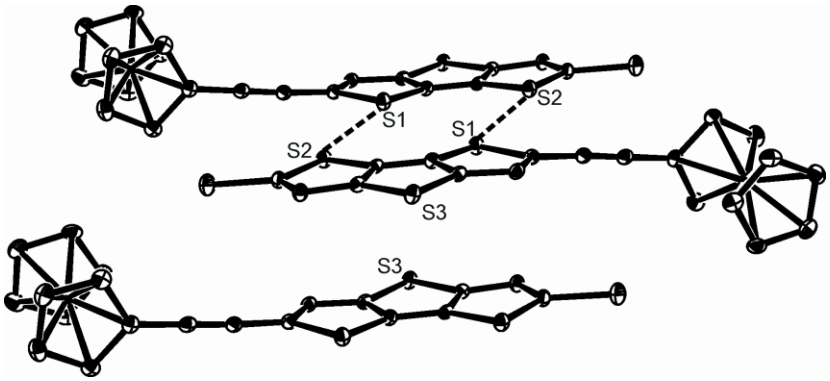

Figure 4. The structure of **8** showing (a, top) the asymmetric unit and the labeling scheme used in the text and (b, bottom) dimerization *via* short S…S contacts; thermal ellipsoids are at the 30% level. Selected geometric data: Fe(1)-C(1,5) ring centroid 1.6497(19), Fe(1)-C(6,10) ring centroid 1.6428(18), C(8)-C(11) 1.435(5), C(12)-C(11) 1.182(5), C(13)-C(12) 1.426(5), S(1)-C(16) 1.719(4), S(1)-C(13) 1.758(4), S(3)-C(15) 1.741(4), S(3)-C(18) 1.743(4), S(2)-C(20) 1.723(4), S(2)-C(17) 1.722(3), Br(1)-C(20) 1.867(4), S(1)…S(2') 3.322(4) Å; C(12)-C(11)-C(8) 179.7(4), C(11)-C(12)-C(13) 176.6(4) °. Symmetry operation: 1-x, 1-y, 1-z.

Overall, there is little variation in the geometric parameters associated with any putative conjugation across these molecules (Table 3), and, indeed, with similar systems previously reported,[43,44,46,47] save for the fact that data for **2** shows potentially the greatest delocalization of π-electron density between metal centers. This is supported by the IR data, which show a much lower ν(C≡C) for **2** (2148 cm^{-1}) than the other complexes structurally characterized (2184 – 2199 cm^{-1}).There are differences in the relative orientations (in the solid state) of Fc moieties at either end of the molecule, between those which are *anti* (**2**, **5**) and those which are orthogonal (**4**, **6**, **8**) though in all these latter cases there are significant intermolecular contacts which conceivably cause reorientation of the Fc units to accommodate packing.

Electrochemistry and Spectro-electrochemistry

Cyclic voltammograms for the oxidation of *bis*-(ferrocenylethynyl) complexes **2-7** and mono(ferrocenylethynyl) complex **8** in dichloroethane (DCE) were recorded as a function of scan rate (20-1000 mVs^{-1}) and over a 0 to 1 V potential range. All complexes were reversibly oxidized as expected for mono- or *bis*-(ferrocenylethynyl) derivatives connected *via* conjugated spacers[29,30] (see Figure 5). $E_{1/2}$ values ranging from 610 mV to 750 mV for the current series (compare for ferrocene $E_{1/2}$ = 0.527 V) indicate the electron withdrawing nature of the spacers (see Table 4). Two clearly resolved overlapping oxidation waves were observed in case of complex **2** (Figure 5(A)) with a separation of ca. $\Delta E_{1/2}$ = 105 mV [here $\Delta E_{1/2} = E_{1/2}^{II} - E_{1/2}^{I}$) with the midpoint potential $E_{1/2} = 0.5(E_{p,ox} + E_{p,red})$]. This indicates a moderately strong electronic interaction between the two Fe atoms, which is not surprising given the shorter Fe-Fe distance (9.597 Å) and good conjugation in this case.

For complexes **3-7** broadened CV peaks without significant splitting of mid-point potentials were observed under similar conditions (see Figure 5). This could result from considerably longer Fe-Fe distance i.e. around ~14 Å. Several studies have shown that substantial electronic interaction may still occur in cases where conjugated organic spacers are used to link the metal centers. Swager reported that redox-matching between the metal and organic components in several transition-metal containing conjugated polymers resulted in enhanced conductivities despite the absence of peak separation in the metal redox waves.[9,77-79]

Table 4. Electrochemical data in mV *vs*. SCE for complexes **2-8** obtained from voltammograms in DCE containing 0.1 M [*n*-Bu_4N]PF_6, ca. 20°C (errors are estimated).

Complex	$E_{1/2}^{I}$ ±5 (mV)	[a]$E_{1/2}^{II}$ ±5 (mV)	$\Delta E_{1/2}$ ±5 (mV)	IVCT band width at ½ height (cm^{-1})	ε_{IVCT}, L mol^{-1} cm^{-1}
2	645	750	105	2364	212
3	612	667	55	2512	478
4	630	740[b]	110	1988	542
5	650	720	70	*c*	*c*
6	650	730[b]	80	*c*	*c*
7	620	672	52	2843[d]	441[d]
8	610	*e*	*e*	*e*	*e*

[a]Values obtained from digital simulation of the cyclic voltammograms. [b]Estimated values from digital simulation in presence of unknown impurity. [c] Due to limited spectral window IVCT band could not be located. [d]IVCT band in part outside the analysis range thus band width estimate reported. [e]Mono(ferrocenylethynyl) complex.

Some other reports have also shown substantial electronic interactions even in the absence of any observable peak separation. For example, despite a small $Ru^{II/III}$ peak separations in the voltammetry, the hybrid metallopolymers bearing bis(2,2′-bipyridyl)Ru moieties on a conjugated backbone[80,81] showed electron diffusion coefficients greater than those for comparable non-conjugated materials by an order of magnitude. Broad CV peaks similar to those of complexes**3-7** have been reported for ferrocenylethynyl poly-ynes and oligo-ynes and the broadening is attributed to the presence of closely spaced redox processes.[82-84]

To investigate the extent of broadening of the CV peaks in complexes **3-7** the CV features were reproduced by digital simulation with Digisim™ (see Figure 5). Successful simulations of the

main features in experimental CVs showed that the broadening in the CV peaks can be reconciled with the presence of two individual, closely spaced, one-electron processes. Figure 5 documents the agreement between the experimental and the simulated CVs for the bis(ferrocenylethynyl) complexes **2, 3, 5** and **7**. The simulation CVs for complexes **4** and **6** (not shown here) had minor additional, and so far unidentified, impurity oxidation peaks.

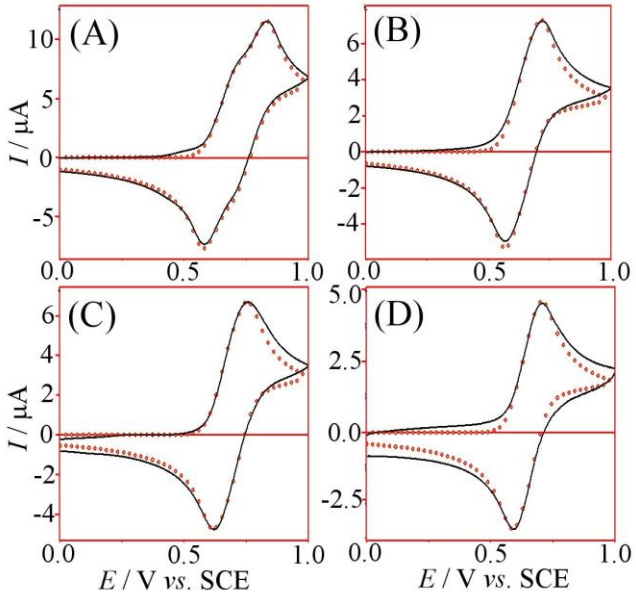

Figure 5. Simulation curves (red circles) matched with cyclic voltammograms (black line) for bis(ferrocenylethynyl) complexes **2**(A), **3**(B), **5**(C) & **7**(D) in DCE at 25°C with 0.1 M [*n*-Bu_4N]PF_6 as supporting electrolyte and at scan rate 100 mVs^{-1}.

A recent report demonstrated significant electronic communication in bis(ferrocenyl) complexes separated by electron withdrawing spacers and having Fe-Fe distance <8Å.[16] Interestingly, **2**, which has the Fe-Fe distance 9.597 Å, and **4,** which has the Fe-Fe distance 13.494 Å, still exhibit similar $\Delta E_{1/2}$ i.e. 105 mV and 110 mV, respectively, which is not too dissimilar compared to values for *para*-diferrocenylbenzene.[28] The electron withdrawing nature of the spacer could have an impact on the net conjugation effect over-riding the Fe-Fe distance effect in this particular

comparison. Other bimetallic complexes supported by bis(NHC) ligands exhibit weaker interactions ($\Delta E_{1/2}$ = 42−80 mV) despite having direct metal-NHC connections and metal-metal distances of less than 11 Å.[82] $\Delta E_{1/2}$ values of 80 mV and 70 mV were found for **6** and **5**, although they have similar Fe-Fe distances as complex **4**. This can be explained by the fact that the connecting unit in **5** and **6** is substituted thiophene which is less conjugated than the substituted benzene unit in complex **4.** Recent reports suggest that electron withdrawing spacers play an important role in the communication of the terminal ferrocene units.[16,85,86] This is reflected in the $\Delta E_{1/2}$ values for complexes **2-7** which range from 50 to 110 mV. While there is no clear relation between the half-wave potential splitting and the strength of the electronic interaction between coupled redox sites[87,88] the values of $\Delta E_{1/2}$ (Table 4) suggest that they belong to Class II according to the Robin and Day classification scheme[89] with modest coupling.

UV-vis spectra were recorded at different applied potentials for complexes **2-8**. An initial spectrum was collected in an OTTLE cell without applying any potential and a series of spectra were then collected by gradually changing the applied potential. The spectra collected in the proximity of the $E_{1/2}^{I}$ value were used for deconvolution to obtain a pure spectrum of the mono-cationic species (see experimental). Figure 6 summarizes neutral and mono-cation spectra as well as showing difference spectra where weak bands are more clearly resolved. The oxidation of complexes **2-8** resulted in strong absorption bands with λ_{max} in the range 260 - 310 nm assigned to π - π^* transition in the organic spacer groups. The shoulder at ~440 - ~570 nm in these spectra is due to $Cp \rightarrow Fe^{III}$ ligand-to-metal charge-transfer (LMCT) band and has been reported for related compounds.[90,91] The broad absorption bands close to the NIR region can be assigned as inter-valence charge transfer (IVCT) bands.

Upon oxidation of **2** to $\mathbf{2}^{+}$, the intensity of the low energy MLCT bands at 395 nm decreases, while the intensity of the higher energy, predominantly π - π* band, increases. In addition, new broad bands at 551 nm and ~766 nm appear in the spectrum. The NIR band was assigned as an IVCT transition. The IVCT nature was confirmed as this band disappears on further oxidation by increasing the potential.[92] Similar observations were found for **3**, where during the spectro-electrochemical oxidation of **3** to $\mathbf{3}^{+}$ the intensity of the low energy MLCT bands at 484 nmdecreases, while the intensity of the higher energyπ - π* band increases; in addition, new bands at 568 nm and 867 nm appear in the spectrum. The former band might consist of overlapping MLCT and LMCT transitions. The NIR was assigned as an IVCT transition (Figure 6(B)). The spectro-electrochemical oxidation of complexes **4-7** are consistent with the data collected for **2** and **3** (Table 1); for **5** and **6** the IVCT bands could not be observed in the spectral window. In Figure 6C (i) and 6C (ii), the spectra of complex **7** and $\mathbf{7}^{+}$ show subtle shifts in the visible absorption, where there is an increase in the intensity of the π - π* band at higher energy and a red shift of the initial MLCT band at 466 nm to a new band at 510 nm. The IVCT band here appears at much longer wavelength ~1020 nm and continues outside the analysis range. The LMCT band at 510 nm for complex **7** can be compared with the LMCT band at 563 nm of the complex **8** i.e. a mono(ferrocenylethynyl) complex with similar spacer group (Figure 6D). This band in **8** is further shifted to lower energy as compared to **7** due to the inductive effect of the terminal bromine. Further, **8** shows a MLCT band at ~760 nm.

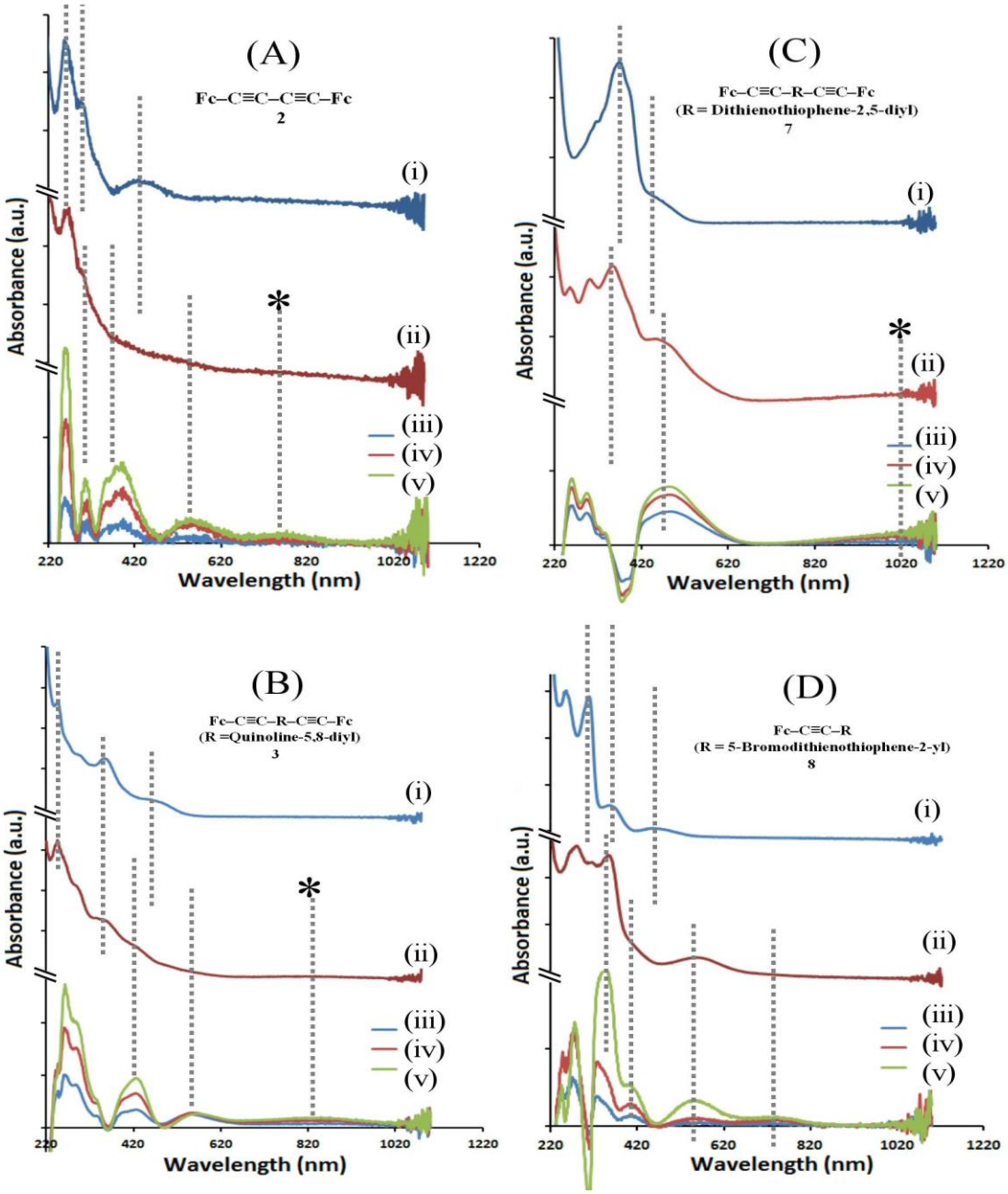

Figure 6. UV-vis spectra of complexes **2-3** and **7-8** in DCE solution at different potentials applied in OTTLE cell with [*n*-Bu_4N]PF_6 as supporting electrolyte (data for the neutral spectra (i), the mono-cation (ii), and difference spectra (iii-v) are shown). (A) **2** (i) neutral (ii) 650 mV; (iii-v) 540, 650 & 710 mV; (B) **3** (i) neutral (ii) 620 mV; (iii-v) 580, 620 & 660 mV;(C) **7** (i) neutral (ii) 630 mV; (iii-v) 600, 630 & 660 mV; and (D) **8** (i) neutral (ii) 650 mV; (iii-v) 620, 650 & 690 mV, respectively.

It is interesting to compare optical and electrochemical data. A stronger intra-molecular interaction should correspond to an increased $\Delta E_{1/2}$, but also the IVCT band oscillator strength given by $4.6 \times 10^{-9} \times \varepsilon_{max} \times \Delta\nu_{1/2}$ (ε_{max} is the extinction coefficient maximum and $\Delta\nu_{1/2}$ is the half width of the IVCT band[93]) should increase. However, this predicted trend cannot be confirmed here. As the $\Delta E_{1/2}$ value increases the IVCT band width appears to decrease, which suggests lower oscillator strength at assumed similar extinction maxima. For example, in the series of complexes **3**, **2**, and **4** the $\Delta E_{1/2}$ values increase 50 mV, 105 mV, 110 mV, but the IVCT band width at half height decreases as 2512, 2364 and 1988 cm^{-1}. Clearly structural effects introduced by the spacer system and additional configurational changes in solution could add complexity and limit the applicability of the $\Delta E_{1/2}$ oscillator strength correlation. Further experimental work, in particular taking into account solvent polarity effects, will be desirable.

Computational studies

IR and structural analysis indicated that complex **2** may potentially have the greatest delocalization of π-electron density between metal centers. The electrochemistry results, $\Delta E_{1/2}$ = 105 mV for complex **2** comparable to complex **4** ($\Delta E_{1/2}$ = 110 mV) motivated us to select complexes **2** and **4** to conduct computational studies to get a better insight into the intramolecular interaction processes. We have therefore attempted to model the delocalization between metals computationally using the B3LY [94] hybrid density functional under the Gaussian09 package [95] for complexes **2** and **4**. The SDD pseudopotential and associated basis set [96] was used for iron, and the 6-31G(d) [97] basis set was used for all other atoms. Geometry optimisations were performed and frequency calculations were used to confirm that the stationary points were true minima; pictures of the HOMOs for **2** and **4** are given in Figure 7. For **2** the HOMO shows

extensive delocalization across the whole molecule, with contributions of 26 (Fe), 11 (C_5H_4) and 23% (C≡C-C≡C) from the contributing fragments. Similarly, the HOMO for **4** (Fig 7, right), though less symmetrical than for **2**, has contributions of 33, 20 (Fe, Fe), 11, 8 (C_5H_4, C_5H_4). 7, 7% (C≡C, C≡C) and 14% (C_6NSN).

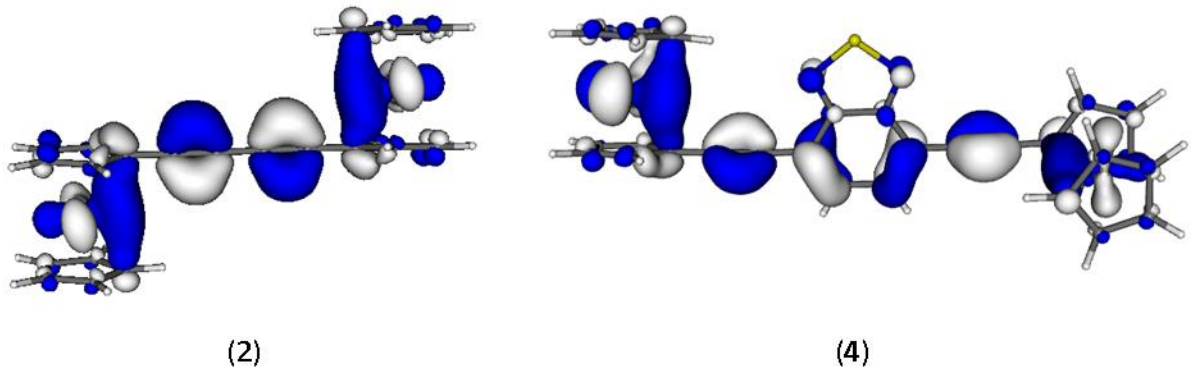

Figure 7. HOMO of **2** (left) and **4** (right)

Conclusion

We have successfully established a synthetic protocol for bis(ferrocenylethynyl) complexes **3-7** and mono(ferrocenylethynyl) complex **8** and characterized these complexes using NMR, IR, Mass, UV-vis spectroscopy. Complexes **4-6** and **8** were characterized by X-ray crystallography. Redox properties of these complexes were investigated using cyclic voltammetry approach and digital simulation revealing two one-electron oxidation processes with difference ranging from 50 to 110 mV. Spectro-electrochemistry performed in an OTTLE cell gave clear indication of formation of mono-cationic species. The appearance of IVCT bands for complexes **2 – 4** and **7** further confirms the mono-cationic species. This work is an example of longer range electronic interaction where the Fe-Fe distance is ~14Å and the spacer is electron withdrawing. Ciomputational studies show there is significant electron delocalization between iron centres in the HOMO of both **2** and **4**. It is demonstrated that the conjugated spacer is important in tuning

the optical and redox property of the bis-ferrocenylethynyl complexes. The results obtained have important implications for the design and synthesis of the metal-containing conjugated poly-ynes and oligo-ynes.

Acknowledgements

We acknowledge the Sultan Qaboos University, Oman for a Research Grant and for a research leave to MSK. HHS and RAAl-B acknowledge Sultan Qaboos University, Oman for PhD scholarships. We are grateful to the British Council for a PMI-2 Grant (GS 216) that has supported MSK, MKAl-S, HHS, PRR and KCM. PRR gratefully acknowledges support from the EPSRC through the award of a Senior Fellowship. We would also like to thank Dr. Dariusz Matoga of Jagiellonian University, Poland for helpful discussion on some cyclicvoltammetry data.

Supporting Information

Crystallographic data for the structural analysis (in CIF format) have been deposited with the Cambridge Crystallographic Data Center, CCDC nos. 610675 – 610679 for **2**, **4** - **6** and **8**, respectively. Copies of this information may be obtained from the Director, CCDC, 12 Union Road, Cambridge, CB21EZ, UK (Fax: +44-1233-336033; e-mail: deposit@ccdc.cam.ac.uk or www.ccdc.cam.ac.uk). This material is available free of charge via the Internet at http://pubs.acs.org.

References

(1) Whittell, G. R.; Hager, M. D.; Schubert, U. S.; Manners, I. *Nat Mater* **2011**, *10*, 176.
(2) Burroughes, J. H.; Bradley, D. D. C.; Brown, A. R.; Marks, R. N.; Mackay, K.; Friend, R. H.; Burns, P. L.; Holmes, A. B. *Nature* **1990**, *347*, 539.
(3) Kraft, A.; Grimsdale, A. C.; Holmes, A. B. *Angew. Chem., Int. Ed.* **1998**, *37*, 402.
(4) Montali, A.; Smith, P.; Weder, C. *Synth. Met.* **1998**, *97*, 123.
(5) Tessler, N.; Denton, G. J.; Friend, R. H. *Nature* **1996**, *382*, 695.
(6) Meier, H. *Angew. Chem. Int. Ed.* **1992**, *31*, 1399.
(7) Halls, J. J. M.; Walsh, C. A.; Greenham, N. C.; Marseglia, E. A.; Friend, R. H.; Moratti, S. C.; Holmes, A. B. *Nature* **1995**, *376*, 498.
(8) Köhler, A.; Wittmann, H. F.; Friend, R. H.; Khan, M. S.; Lewis, J. *Synth. Met.* **1994**, *67*, 245.
(9) Köhler, A.; Wittmann, H. F.; Friend, R. H.; Khan, M. S.; Lewis, J. *Synth. Met.* **1996**, *77*, 147.
(10) Swager, T. M. *Acc. Chem. Res.* **1998**, *31*, 201.
(11) Khan, M. S.; Al-Suti, M. K.; Shah, H. H.; Al-Humaimi, S.; Al-Battashi, F. R.; Bjernemose, J. K.; Male, L.; Raithby, P. R.; Zhang, N.; Kohler, A.; Warren, J. E. *Dalton Trans.* **2011**, *40*, 10174.
(12) Ho, C.-L.; Wong, W.-Y. *Coord. Chem. Rev.* **2011**, *255*, 2469.
(13) Wong, W.-Y.; Ho, C.-L. *Acc. Chem. Res.* **2010**, *43*, 1246.
(14) Wong, W.-Y.; Harvey, P. D. *Macromol. Rapid Commun.* **2010**, *31*, 671.
(15) Wong, W.-Y.; Ho, C.-L. *Coord. Chem. Rev.* **2006**, *250*, 2627.
(16) Solntsev, P. V.; Dudkin, S. V.; Sabin, J. R.; Nemykin, V. N. *Organometallics* **2011**, *30*, 3037.
(17) Santi, S.; Orian, L.; Donoli, A.; Bisello, A.; Scapinello, M.; Benetollo, F.; Ganis, P.; Ceccon, A. *Angew. Chem., Int. Ed.* **2008**, *47*, 5331.
(18) Astruc, D.; Ornelas, C.; Ruiz Aranzaes, J. *J. Inorg. Organomet. Polym. Mater.* **2008**, *18*, 4.
(19) Wagner, M. *Angew. Chem., Int. Ed.* **2006**, *45*, 5916.
(20) Barlow, S.; O'Hare, D. *Chem. Rev.* **1997**, *97*, 637.
(21) Kaifer, A. E. *Eur. J. Inorg. Chem.* **2007**, 5015.
(22) Barlow, S. *Inorg. Chem.* **2001**, *40*, 7047.
(23) Debroy, P.; Roy, S. *Coord. Chem. Rev.* **2007**, *251*, 203.
(24) Thomas, K. R. J.; Lin, J. T.; Wen, Y. S. *Organometallics* **2000**, *19*, 1008.
(25) Yin, J.; Yu, G.-A.; Tu, H.; Liu, S. H. *Appl. Organomet. Chem.* **2006**, *20*, 869.
(26) Auger, A.; Swarts, J. C. *Organometallics* **2007**, *26*, 102.
(27) Nemykin, V. N.; Hadt, R. G. *J. Phys. Chem. A* **2010**, *114*, 12062.
(28) Low, P.; Roberts, R.; Cordiner, R.; Hartl, F. *J. Solid State Electrochem.* **2005**, *9*, 717.
(29) Zhu, Y.; Wolf, M. O. *J. Am. Chem. Soc.* **2000**, *122*, 10121.
(30) Diallo, A. K.; Daran, J.-C.; Varret, F.; Ruiz, J.; Astruc, D. *Angew. Chem., Int. Ed.* **2009**, *48*, 3141.
(31) Yuan, Y.-F.; Cardinaels, T.; Lunstroot, K.; Van Hecke, K.; Van Meervelt, L.; Görller-Walrand, C.; Binnemans, K.; Nockemann, P. *Inorg. Chem.* **2007**, *46*, 5302.
(32) Tanaka, Y.; Inagaki, A.; Akita, M. *Chem. Commun.* **2007**, 1169.
(33) Warren, M. R.; Brayshaw, S. K.; Hatcher, L. E.; Johnson, A. L.; Schiffers, S.; Warren, A. J.; Teat, S. J.; Warren, J. E.; Woodall, C. H.; Raithby, P. R. *Dalton Trans.* **2012**, *41*, 13173.

(34) Saha, R.; Qaium, M. A.; Debnath, D.; Younus, M.; Chawdhury, N.; Sultana, N.; Kociok-Kohn, G.; Ooi, L.-l.; Raithby, P. R.; Kijima, M. *Dalton Trans.* **2005**, 2760.
(35) Wilson, J. S.; Chawdhury, N.; Al-Mandhary, M. R. A.; Younus, M.; Khan, M. S.; Raithby, P. R.; Köhler, A.; Friend, R. H. *J. Am. Chem. Soc.* **2001**, *123*, 9412.
(36) Markwell, R. D.; Butler, I. S.; Kakkar, A. K.; Khan, M. S.; Al-Zakwani, Z. H.; Lewis, J. *Organometallics* **1996**, *15*, 2331.
(37) de la Riva, H.; Nieuwhuyzen, M.; Mendicute Fierro, C.; Raithby, P. R.; Male, L.; Lagunas, M. C. *Inorg. Chem.* **2006**, *45*, 1418.
(38) Pintado-Alba, A.; de la Riva, H.; Nieuwhuyzen, M.; Bautista, D.; Raithby, P. R.; Sparkes, H. A.; Teat, S. J.; Lopez-de-Luzuriaga, J. M.; Lagunas, M. C. *Dalton Trans.* **2004**, 3459.
(39) Li, P.; Ahrens, B.; Bond, A. D.; Davies, J. E.; Koentjoro, O. F.; Raithby, P. R.; Teat, S. J. *Dalton Trans.* **2008**, 1635.
(40) Li, P.; Ahrens, B.; Feeder, N.; Raithby, P. R.; Teat, S. J.; Khan, M. S. *Dalton Trans.* **2005**, 874.
(41) Cuffe, L.; Hudson, R. D. A.; Gallagher, J. F.; Jennings, S.; McAdam, C. J.; Connelly, R. B. T.; Manning, A. R.; Robinson, B. H.; Simpson, J. *Organometallics* **2005**, *24*, 2051.
(42) Justin Thomas, K. R.; Lin, J. T.; Wen, Y. S. *Organometallics* **2000**, *19*, 1008.
(43) Chawdhury, N.; Long, N. J.; Mahon, M. F.; Ooi, L.-l.; Raithby, P. R.; Rooke, S.; White, A. J. P.; Williams, D. J.; Younus, M. *J. Organomet. Chem.* **2004**, *689*, 840.
(44) Wong, W.-Y.; Ho, K.-Y.; Choi, K.-H. *J. Organomet. Chem.* **2003**, *670*, 17.
(45) Rodriguez, J.-G.; Oñate, A.; Martin-Villamil, R. M.; Fonseca, I. *J. Organomet. Chem.* **1996**, *513*, 71.
(46) Wong, W.-Y.; Ho, K.-Y.; Ho, S.-L.; Lin, Z. *J. Organomet. Chem.* **2003**, *683*, 341.
(47) Wong, W.-Y.; Lu, G.-L.; Ng, K.-F.; Wong, C.-K.; Choi, K.-H. *J. Organomet. Chem.* **2001**, *637–639*, 159.
(48) Wong, W.-Y.; Lu, G.-L.; Choi, K.-H.; Guo, Y.-H. *J. Organomet. Chem.* **2005**, *690*, 177.
(49) Wong, W.-Y.; Lu, G.-L.; Ng, K.-F.; Choi, K.-H.; Lin, Z. *J. Chem. Soc., Dalton Trans.* **2001**, *0*, 3250.
(50) Bruce, M. I.; Low, P. J.; Hartl, F.; Humphrey, P. A.; de Montigny, F.; Jevric, M.; Lapinte, C.; Perkins, G. J.; Roberts, R. L.; Skelton, B. W.; White, A. H. *Organometallics* **2005**, *24*, 5241.
(51) Tanaka, Y.; Ishisaka, T.; Inagaki, A.; Koike, T.; Lapinte, C.; Akita, M. *Chem. Eur. J.* **2010**, *16*, 4762.
(52) McAdam, C. J.; Cameron, S. A.; Hanton, L. R.; Manning, A. R.; Moratti, S. C.; Simpson, J. *CrystEngComm* **2012**, *14*, 4369.
(53) Morisaki, Y.; Murakami, T.; Chujo, Y. *J. Inorg. Organomet. Polym.* **2009**, *19*, 104.
(54) Wang, Q.; Wong, W.-Y. *Polymer Chemistry* **2011**, *2*, 432.
(55) Dai, F.-R.; Zhan, H.-M.; Liu, Q.; Fu, Y.-Y.; Li, J.-H.; Wang, Q.-W.; Xie, Z.; Wang, L.; Yan, F.; Wong, W.-Y. *Chem. Eur. J.* **2012**, *18*, 1502.
(56) Wang, X.-Z.; Wang, Q.; Yan, L.; Wong, W.-Y.; Cheung, K.-Y.; Ng, A.; Djurišić, A. B.; Chan, W.-K. *Macromol. Rapid Commun.* **2010**, *31*, 861.
(57) He, G.; Yan, N.; Cui, H.; Liu, T.; Ding, L.; Fang, Y. *Macromol.* **2011**, *44*, 7096.
(58) Saito, N.; Kanbara, T.; Nakamura, Y.; Yamamoto, T.; Kubota, K. *Macromol.* **1994**, *27*, 756.
(59) Tokoro, Y.; Nagai, A.; Kokado, K.; Chujo, Y. *Macromol.* **2009**, *42*, 2988.

(60) Wong, W.-Y.; Wang, X.-Z.; He, Z.; Djurisic, A. B.; Yip, C.-T.; Cheung, K.-Y.; Wang, H.; Mak, C. S. K.; Chan, W.-K. *Nat Mater* **2007**, *6*, 521.
(61) Nietfeld, J. P.; Schwiderski, R. L.; Gonnella, T. P.; Rasmussen, S. C. *J. Org. Chem.* **2011**, *76*, 6383.
(62) Kenning, D. D.; Mitchell, K. A.; Calhoun, T. R.; Funfar, M. R.; Sattler, D. J.; Rasmussen, S. C. *J. Org. Chem.* **2002**, *67*, 9073.
(63) Zhou, E.; Cong, J.; Yamakawa, S.; Wei, Q.; Nakamura, M.; Tajima, K.; Yang, C.; Hashimoto, K. *Macromol.* **2010**, *43*, 2873.
(64) Roncali, J. *Chem. Rev.* **1992**, *92*, 711.
(65) Luo, S.-J.; Liu, Y.-H.; Liu, C.-M.; Liang, Y.-M.; Ma, Y.-X. *Synth. Commun.* **2000**, *30*, 1569.
(66) Rosenblum, M.; Brawn, N.; Papenmeier, J.; Applebaum, M. *J. Organomet. Chem.* **1966**, *6*, 173.
(67) Khan, M. S.; Al-Suti, M. K.; Al-Mandhary, M. R. A.; Ahrens, B.; Bjernemose, J. K.; Mahon, M. F.; Male, L.; Raithby, P. R.; Friend, R. H.; Kohler, A.; Wilson, J. S. *Dalton Trans.* **2003**, 65.
(68) Younus, M.; Köhler, A.; Cron, S.; Chawdhury, N.; Al-Mandhary, M. R. A.; Khan, M. S.; Lewis, J.; Long, N. J.; Friend, R. H.; Raithby, P. R. *Angew. Chem., Int. Ed.* **1998**, *37*, 3036.
(69) Sheldrick, G. M. *Acta Crystallogr., Sect. A: Found. Crystallogr.* **1990**, *46*, 467.
(70) Sheldrick, G. M. *Acta Crystallogr., Sect. A.* **2008**, *64*, 112.
(71) Neudeck, A.; Kress, L. *J. Electroanal. Chem.* **1997**, *437*, 141.
(72) Shamsipur, M.; Hemmateenejad, B.; Babaei, A.; Faraj-Sharabiani, L. *J. Electroanal. Chem.* **2004**, *570*, 227.
(73) Yamada, Y.; Mizutani, J.; Kurihara, M.; Nishihara, H. *J. Organomet. Chem.* **2001**, *637–639*, 80.
(74) Keesey, R. L.; Ryan, M. D. *Anal. Chem.* **1999**, *71*, 1744.
(75) Khan, M. S.; Al-Suti, M. K.; Al-Mandhary, M. R. A.; Ahrens, B.; Bjernemose, J. K.; Mahon, M. F.; Male, L.; Raithby, P. R.; Friend, R. H.; Kohler, A.; Wilson, J. S. *Dalton Trans.* **2003**, 65.
(76) Huang, P.; Jin, B.; Liu, P.; Cheng, L.; Cheng, W.; Zhang, S. *J. Organomet. Chem.* **2012**, *697*, 57.
(77) Zhu, S. S.; Carroll, P. J.; Swager, T. M. *J. Am. Chem. Soc.* **1996**, *118*, 8713.
(78) Zhu, S. S.; Swager, T. M. *J. Am. Chem. Soc.* **1997**, *119*, 12568.
(79) Kingsborough, R. P.; Swager, T. M. *Adv. Mater.* **1998**, *10*, 1100.
(80) Cameron, C. G.; Pickup, P. G. *J. Am. Chem. Soc.* **1999**, *121*, 11773.
(81) Cameron, C. G.; Pickup, P. G. *Chem. Commun.* **1997**, 303.
(82) Mercs, L.; Neels, A.; Albrecht, M. *Dalton Trans.* **2008**, 5570.
(83) Reddinger, J. L.; Reynolds, J. R. *Macromol.* **1997**, *30*, 673.
(84) Plenio, H.; Hermann, J.; Sehring, A. *Chem. Eur. J.* **2000**, *6*, 1820.
(85) Chen, Y. J.; Pan, D. S.; Chiu, C. F.; Su, J. X.; Lin, S. J.; Kwan, K. S. *Inorg. Chem.* **2000**, *39*, 953.
(86) Chung, M.-C.; Gu, X.; Etzenhouser, B. A.; Spuches, A. M.; Rye, P. T.; Seetharaman, S. K.; Rose, D. J.; Zubieta, J.; Sponsler, M. B. *Organometallics* **2003**, *22*, 3485.
(87) Mücke, P.; Linseis, M.; Záliš, S.; Winter, R. F. *Inorg. Chim. Acta* **2011**, *374*, 36.
(88) Maurer, J.; Winter, R.; Sarkar, B.; Záliš, S. *J. Solid State Electrochem.* **2005**, *9*, 738.

(89) Robin, M. B.; Day, P. *Adv. Inor. chem* **1968**, *Volume 10*, 247.
(90) Zhu, Y. B.; Wolf, M. O. *Chem. Mater.* **1999**, *11*, 2995.
(91) Sohn, Y. S.; Hendrickson, D. N.; Gray, H. B. *J. Am. Chem. Soc.* **1971**, *93*, 3603.
(92) Levanda, C.; Bechgaard, K.; Cowan, D. O. *J. Org. Chem.* **1976**, *41*, 2700.
(93) Hildebrandt, A.; Schaarschmidt, D.; Claus, R.; Lang, H. *Inorg. Chem.* **2011**, *50*, 10623.
(94) (a) Becke, A. D. *J. Chem. Phys.* **1993**, *98*, 5648. (b) Lee, C. T.; Yang, W. T.; Parr, R. G. *Phys. Rev. B* **1988**, *37*, 785.
(95). M. J. Frisch *et al*., Gaussian 03, Revision D.01., Gaussian, Inc., Wallingford CT, 2004.
(96) Andrae, D.; Haussermann, U.; Dolg, M.; Stoll, H.; Preuss, H. *Theoretica Chim. Acta* **1990**, *77*, 123.
(97) (a) Ditchfield, R.; Hehre, W. J.; Pople, J. A. *J. Chem. Phys.* **1971**, *54*, 724. (b) Hariharan, P. C.; Pople, J. A. *Theoretica Chim. Acta* **1973**, *28*, 213.

Graphical Abstract

Long range intra-molecular electronic communication in bis-(ferrocenyl-ethynyl) complexes incorporating conjugated heterocyclic spacers : synthesis, crystallography and electrochemistry

Hakikulla H. Shah,[a] Rayya A. Al-Balushi,[a] Mohammed K. Al-Suti,[a] Muhammad S. Khan,[a]* Christopher H. Woodall,[b] Kieran C. Molloy,[b] Paul R. Raithby,[b]* Thomas P. Robinson, bSara E. C. Dale,[b] Frank Marken[b]*

[a] Department of Chemistry, Sultan Qaboos University, P.O. Box 36, Al-Khodh 123, Sultanate of Oman

[b] Department of Chemistry, University of Bath, Bath BA2 7AY, UK.

A series of bis-(ferrocenyl-ethynyl) complexes in which the iron centres communicate *via* a range of conjugated heterocylic spacers have been synthesised and the interaction between metals probed by spectro-electrochemical methods.